Computational Materials Science 144 (2018) 161–169

Contents lists available at ScienceDirect

Computational Materials Science

journal homepage: www.elsevier.com/locate/commatsci

# Kapitza conductance of symmetric tilt grain boundaries of monolayer boron nitride

Mohan S.R. Elapolu, Alireza Tabarraei *

*Department of Mechanical Engineering & Engineering Science, University of North Carolina at Charlotte, Charlotte, NC 28223, United States*

ARTICLE INFO

*Article history:*
Received 14 August 2017
Received in revised form 17 November 2017
Accepted 11 December 2017

*Keywords:*
H–BN
RNEMD
Grain boundary
Kapitza conductance

ABSTRACT

We use reverse nonequilibrium molecular dynamics simulations to study thermal conductivity of two–dimensional hexagonal boron nitride (h–BN) nanoribbons containing symmetric tilt grain boundaries. The simulations are conducted on periodic h–BN nanoribbons with zigzag and armchair chirality. The effective thermal conductivity of ribbons and Kapitza conductance of grain boundaries are calculated by inducing a constant heat flux along the longitudinal direction of ribbons. The steady state temperature profiles of nanoribbons display jumps at the location of grain boundaries. The temperature jumps monolithically increases with the misorientation angle of grain boundaries indicating that grain boundaries with higher misorientation angle have lower Kapitza conductance. The lower Kapitza conductance is due to higher phonon scattering at grain boundaries which is a result of a higher mismatch between the phonon spectra of grain boundary and grain atoms. Our modeling results also predict that by increasing the length, both Kapitza conductance of grain boundaries and effective thermal conductivity of ribbons increases. Although temperature does not have a significant impact on Kapitza conductance, but by increasing temperature effective thermal conductivity of ribbons decreases.



## 1. Introduction

Monolayer hexagonal boron nitride (h–BN) is a graphene–like two–dimensional material which has a honeycomb lattice structure containing an equal number of B and N atoms covalently bonded in alternating sites [1–3]. Two–dimensional hexagonal boron nitride displays excellent thermal conductivity [4–7], remarkable mechanical strength [8–11] and excellent optical properties [12–14]. Such remarkable properties make h–BN promising for various applications including nanoscale electronics [15–18], optoelectronic [19], electrochemical sensing devices [20] and composite materials [21–24]. Using h–BN for such applications requires large scale synthesis of h–BN. Chemical vapor deposition (CVD) is the prominent method used for large scale synthesis of nanomaterials such as h–BN [25–27]. Hexagonal boron nitride sheets obtained using CVD are polycrystalline consisting of individual grains stitched at grain boundaries [28]. Grain boundaries act as extended defects and their presence can significantly affect the properties of h–BN. The structure of grain boundaries and their impact on the thermal properties of bulk materials have been extensively investigated in the past [29,30]. Studies on the effect of grain boundaries on the properties of two–dimensional materials are mostly limited to graphene [31–33] and the impact of grain boundaries on the properties of other two–dimensional materials are rarely studied.

High thermal conductivity of h–BN makes it important for diverse applications such as thermal management in electronics and thermal conductance enhancement of composite materials. Since grain boundaries are inevitably present in h–BN sheets, studying the impact of such defects on heat transport in h–BN is necessary. Such investigations not only reveal unique features regarding heat transport mechanism at nanoscale, but can provide insights on using defect engineering as a way for tailoring the thermal conductivity of h–BN.

Due to challenges in conducting experiments at nanoscale, computational methods have become invaluable tools for studying properties of two–dimensional materials [34–42]. We use reverse nonequilibrium molecular dynamics (RNEMD) methods to study the impact of grain boundaries on the thermal conductivity of armchair and zigzag h–BN nanoribbons containing symmetric tilt grain boundaries. To understand the impact of the structure of grain boundaries on their thermal properties, grain boundaries with different misorientation angles are studied. Using phonon spectrum density of grains and grain boundaries we show that phonon scattering at grain boundaries is responsible for the thermal resistance

* Corresponding author.
*E-mail address:* atabarra@uncc.edu (A. Tabarraei).

https://doi.org/10.1016/j.commatsci.2017.12.019
0927-0256/

at grain boundaries. By increasing the misorientation angle, Kapitza conductance of ribbons reduce which leads to a lower effective thermal conductivity of ribbons as well. The effect of temperature and grain size on the thermal properties of h–BN are studied. The modeling results predict that by increasing the length of grains the Kapitza conductance and effective thermal conductivity of ribbons increases. On the other hand, while the impact of temperature on the Kapitza conductance of grain boundaries is negligible, the effective thermal conductivity of ribbons reduces by increasing the temperature.

## 2. The structure of nanoribbons and grain boundaries

The structure of nanoribbons used in this paper for RNEMD modeling is schematically shown in Fig. 1(a). The nanoribbons are periodic in the $x$–direction and each computational cell consists of four similar grain boundaries in the $y$–direction. All the four grains of the computational cell have the same size in the $x$–direction and their width in the $y$–direction is 123 Å. The lattice vectors $\mathbf{a}_1 = \frac{a}{2}(3, \sqrt{3})$ and $\mathbf{a}_2 = \frac{a}{2}(3, -\sqrt{3})$ are shown in Fig. 2(f) where $a \approx 1.4457$ Å [43] is the boron–nitrogen bond length.

The grain boundaries considered in this paper are shown in Figs. 2–4. As shown all the grain boundaries consist of repeating pentagon–heptagon (5–7) pairs [28]. Each 5–7 pair is known as a Stone–Wales defect and represents the core of an edge dislocation corresponding to the removal of one chain of armchair atoms from the perfect lattice. Similar structures have been previously studied for the grain boundary of graphene [44].

As depicted in Fig. 2, the grain boundaries of zigzag ribbons comprised of a regular array of 5–7 Stone–Wales defects separated by hexagonal rings [28]. Increasing the misorientation angle reduces the number of hexagonal rings between 5–7 pairs which is equivalent to increase in the dislocation density. At a misorientation angle of $\theta_{zig} = 21.73°$, the 5–7 pairs are separated by only one hexagonal ring. Therefore, it is not possible to further increase the misorientation angle of grain boundaries while keeping the regular array of 5–7 defects. The Burger vector ($\mathbf{b}$) of edge dislocations can be obtained by plotting Burger circuits around a 5–7 pair as shown in Fig. 2(f). Using the Burger circuit, the Burger vector of dislocations at each Stone–Wales defect of grain boundaries in zigzag ribbons is $\mathbf{b} = \mathbf{a}_1$.

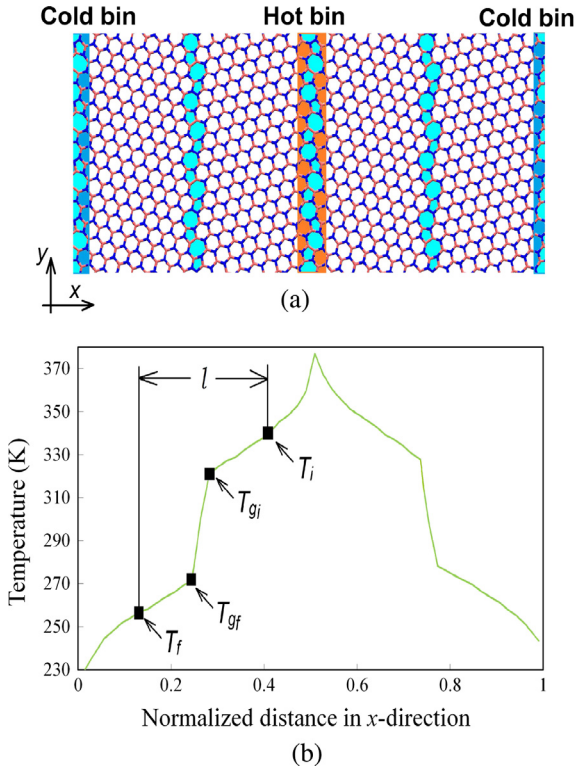


**Fig. 1.** (a) A h–BN nanoribbon containing four similar grain boundaries used in the RNEMD simulations. The hot bin is at the middle and cold bins are at the two ends of the ribbon. (b) The temperature profile of the nanoribbon is shown schematically. The temperature profile includes a jump at the location of grain boundaries.

As shown in Fig. 3, the grain boundaries in armchair ribbons are comprised of two pairs of 5–7 Stone–Wales defects. By plotting the Burger circuit around two 5–7 pairs, as depicted in Fig. 3(f), the Burger vector of the dislocations are obtained as $\mathbf{b} = \mathbf{a}_1 + \mathbf{a}_2$. Similar to grain boundaries in zigzag ribbons, by increasing the misorientation angle, the number of hexagonal rings between two adjacent dislocations reduces. At a misorientation angle of $\theta_{arm} = 27.77°$ the Stone–Wales defects join each other and the hexagonal rings separating the dislocations disappear. Further increase in the misorientation angle will alter the Burger vector of dislocations.

To study the structure of grain boundaries with higher misorientation angle, we note the relation $\theta_{zig} = 60° - \theta_{arm}$. Therefore, the maximum misorientation angle of armchair ribbons observed in Fig. 3, i.e. $\theta_{arm} = 27.77°$ is equivalent to $\theta_{zig} = 32.23°$. Since the maximum misorientation $\theta_{zig}$ in Fig. 2 is 21.73°, the range of $\theta_{zig}$ between 21.73° and 32.23° is a transition zone where the grain boundary dislocations are a combination of those from armchair and zigzag ribbons.

The structure of grain boundaries in the transition zone for two misorientation angles of $\theta_{zig} = 24.43°$ and 27.79° are shown in Fig. 4. As shown in Fig. 4(c–d), the structure of grain boundary in the transition zone is not made of just one type of dislocation. Instead the grain boundaries are comprised of (1,0) and (1,0)+(1,0)+(1,0) dislocations. When the misorientation angle is close to $\theta_{zig} = 21.73°$, the density of (1,0) dislocations is higher than the density of (1,0)+(1,0)+(1,0) dislocations. When the misorientation angle approaches $\theta_{zig} = 32.23°$, i.e, when the misorientation angle get closer to that of armchair ribbons, the (1,0) dislocations disappear and the grain boundary is made of an array of (1,0)+(1,0)+(1,0) dislocations.

In the rest of this paper, to ease the illustration of results, the data related to the grain boundaries in the transition zone, i.e $21.73° < \theta_{zig} < 32.23°$, are presented along with the results of grain boundaries of zigzag ribbons.

## 3. Computational method

In this paper, we use reverse nonequilibrium molecular dynamics (RNEMD) method [45] to study thermal transport in h–BN ribbons containing symmetric tilt grain boundaries. In this method a heat flux in the $x$–direction is imposed to create a temperature gradient in the longitudinal direction of ribbons as shown in Fig. 1(b). For this purpose, the nanoribbon are divided into bins with the first bin is designated as the cold bin and the bin at the middle is designated as the hot bin, as shown in Fig. 1(a). In this paper, the number of bins are chosen based on the length of the ribbons such that the width of bins does not change by the change in the ribbons length. As a reference point, we use 52 bins for ribbons with a length of 750 Å. The heat flux is induced by a continuous transfer of energy from the cold bin to the hot bin. The energy transfer is conducted by exchanging the kinetic energy of the coldest atom of the hot bin with the hottest atom of the cold bin, as shown in Fig. 1(a). The swap of energy is continuously repeated until a steady state temperature profile is obtained. Due to the artificially